Phase Behavior of Block Copolymers in a Neutral Solvent

Timothy P. Lodge,*,†,‡ Kenneth J. Hanley,‡,§ Bryant Pudil,‡,|| and Vindya Alahapperuma‡,⊥

Department of Chemistry and Department of Chemical Engineering & Materials Science, University of Minnesota, Minneapolis, Minnesota 55455-0431

Received June 18, 2002

ABSTRACT: The phase behavior of eight poly(styrene-*b*-isoprene) diblock copolymers in the neutral solvent dioctyl phthalate (DOP) has been examined over the full concentration (ϕ) range and from room temperature up to 250 °C. The copolymer compositions (f) ranged from 0.15 to 0.76, and molecular weights were chosen to make the melt order−disorder transition (ODT) accessible, or nearly so. Definitive phase assignments were made on the basis of small-angle X-ray scattering (SAXS). Individual order−order transitions (OOTs) and ODTs were located by a combination of rheology, static birefringence, and SAXS; all three techniques gave equivalent results. The transition temperatures were converted to values of the effective interaction parameter, χ, using an established relation for this system. For all compositions, χ_{ODT} scales as $\phi^{-\alpha}$, with α varying from 1.3 to 1.6. These results are in conflict with the mean-field dilution approximation ($\alpha = 1.0$), as was previously demonstrated for lamellae-forming samples. This result is attributed to the additional fluctuation stabilization of the disordered state in two-component solutions. Three of the samples displayed OOTs: cylinder to sphere ($f = 0.15$), gyroid to cylinder ($f = 0.31$), and lamellae to gyroid ($f = 0.33$). In each case, χ_{OOT} scaled as $\phi^{-1.0}$, in agreement with the dilution approximation. This result underscores the reliability of mean-field theory for computing relative free energies of the various ordered phases. The domain spacing, d, scales approximately as $\phi^{0.33}$ and $\chi^{0.25}$, independent of morphology, in good agreement with both mean-field theory and previous experiments.

Introduction

The phase behavior of AB diblock copolymers in the bulk has been extensively studied, both experimentally and theoretically, and much of the phenomenology is well understood.[1,2] From an applications perspective, however, block copolymers are generally employed as one component in a mixture, and thus the phase behavior of block copolymers blended with homopolymers and/or low molecular weight diluents is of general relevance. A diluent or solvent can serve many purposes, including controlling the choice of self-assembled structure, tuning the order−disorder transition (ODT) and order−order transition (OOT) temperatures, improving the tack or adhesive properties, and aiding in processing. A solvent may be classified as neutral or selective, depending on the extent to which it preferentially swells the microdomains of the copolymer morphology, and the entire spectrum from neutral to very selective is of interest.

For the particular case of a neutral solvent, there are three general questions: (i) to what extent is the "topology" of the melt phase map preserved upon dilution, (ii) how do the ODT and OOT temperatures scale with concentration, and (iii) how do microdomain composition profiles and dimensions vary with dilution? In the simplest scenario, the solvent would be distributed uniformly throughout the solution, diluting the A/B contacts and lowering the transition temperatures. The essential competition between interfacial tension and chain stretching under the volume-filling constraint, which determines the morphology in the bulk, would be unaltered. This picture corresponds to the "dilution approximation" first introduced by Helfand and Tagami,[3] whereby the effective interaction parameter in the solution, χ_{eff}, is simply given by $\phi\chi$, the product of the polymer volume fraction and A/B interaction parameter. The self-consistent mean-field theory (SCMF), which describes many features of the melt phase behavior remarkably well, has been extended to block copolymer solutions.[4−7] One important result of these calculations is that the phase diagram (i.e., a plot of degree of segregation χN vs copolymer composition, f, where N is the degree of polymerization) is found to be almost identical to the melt, with χ simply replaced by χ_{eff}. There are at least two reasons why this might not be true experimentally. First, it is well-established that non-mean-field fluctuation effects suppress the melt ODT compared to the SCMF calculations.[2,8−10] In solution, the possibility exists for polymer/solvent as well as block/block concentration fluctuations to exacerbate this effect. There is ample experimental evidence for substantial concentration fluctuations in the solution case.[11−13] Second, as ϕ decreases, the individual chains will swell, assuming non-Gaussian conformations not yet accounted for in the SCMF calculations. Theories for χ_{eff} in solutions of polymer mixtures have been extended to block copolymer solutions by Fredrickson and Leibler[14] and by Olvera de la Cruz;[15] in semidilute solutions the scaling $\chi_{eff} \sim \phi^{1.6}\chi$ is anticipated.

We have been conducting a systematic investigation of the block copolymer solution phase diagram, as a function of the relevant variables: N, f, ϕ, and temperature, T, for solvents of varying selectivity.[16−20] Experimentally, we have shown that the dilution approximation fails to describe the concentration dependence of the ODT for lamellar copolymers in neutral good solvents, even at very high concentrations.[16] Furthermore, there is some evidence that the concentration dependence is nonuniversal; for example, in poly(styrene-

* Author for correspondence: e-mail lodge@chem.umn.edu.
† Department of Chemistry.
‡ Department of Chemical Engineering & Materials Science.
§ Current address: 3M Company, St. Paul, MN 55144.
|| Current address: Polymerix Corporation, Voorhees, NJ 08043.
⊥ Current address: Millenium Hotel, Minneapolis, MN.

10.1021/ma0209601 CCC: $25.00
Published on Web 01/07/2003

Table 1. Sample Characteristics

sample	$M_n \times 10^4$	M_w/M_n	N	f	ODTs	OOTs
SI(11−52)	6.3_5	1.04	691	0.15	7	8
SI(11−32)	4.2_5	1.02	456	0.23	7	0
SI(11−21)	3.1_4	1.05	333	0.31	7	6
SI(12−21)	3.2_3	1.04	341	0.33	8	6
SI(15−13)	2.7_6	1.02	285	0.50	6	0
SI(22−12)	3.4_3	1.03	348	0.60	5	0
SI(38−14)	5.2_2	1.01	523	0.70	4	0
SI(50−13)	6.3_0	1.01	626	0.76	4	0

b-isoprene) $\chi_{eff} \sim \phi^{1.6}\chi$ whereas for poly(ethylene propylene-*b*-ethylethylene) $\chi_{eff} \sim \phi^{1.2}\chi$.[16] A liquid-state approach based on the PRISM model is apparently able to capture this phenomenology, although the ODT cannot be located rigorously.[9,10,21] In contrast, for one asymmetric copolymer which exhibited a gyroid → cylinder OOT, we found that the OOT did follow the dilution approximation.[18] Consequently, it is of interest to see whether these phenomena persist for different f. Accordingly, in this paper we describe the phase behavior of eight poly(styrene-*b*-isoprene) diblock copolymers in the neutral solvent dioctyl phthalate. The ODTs and OOTs were located by a combination of small-angle X-ray scattering, rheology, and static birefringence. In all, 48 ODTs (i.e., combinations of ϕ_{ODT} and T_{ODT}) and 20 OOTs were determined. The results are discussed in terms of the three questions posed above.

Experimental Section

Samples and Solutions. Eight poly(styrene-*b*-isoprene) diblock copolymers were prepared by living anionic polymerization, as described previously.[20] Styrene was purified over calcium hydride, followed by vacuum distillation and treatment with *n*-butyllithium. Isoprene was purified with dibutylmagnesium followed by *n*-butyllithium. The polymerization solvent was cyclohexane, which had itself been distilled from *n*-butyllithium. Polymerization was initiated with *sec*-butyllithium and continued at 40 °C for 4 h for each block.

The polymers were characterized by size exclusion chromatography (SEC) with multiangle light scattering detection (Wyatt DAWN) and by proton NMR. The weight-average molecular weight, M_w, and polydispersity, M_w/M_n, were determined for each polymer via light scattering. The samples are denoted SI($X-Y$), where X and Y refer to the PS and PI block molecular weights in kg/mol. The mole fractions of styrene and isoprene repeat units, and the polyisoprene microstructure, were determined by NMR. The degrees of polymerization and the compositions agreed very well with the values calculated on the basis of stoichiometry, assuming complete conversion. The resulting uncertainties are estimated to be 5% in M_w and 0.5% in composition. The PI microstructure was consistently 94 ± 1% 4,1. The compositions were converted to volume fraction of styrene, f, assuming additivity of volumes and densities of 1.05 and 0.913 g/mL for PS and PI, respectively. The degree of polymerization, N, was calculated in terms of a polystyrene reference segment volume. The sample characteristics are listed in Table 1.

Bis(2-ethylhexyl) phthalate, commonly referred to as dioctyl phthalate (DOP), was obtained from Aldrich. The solvent was rigorously purified by washing with 5% aqueous sodium bicarbonate followed by repeated washing with distilled water. Any remaining water and alcohols were removed by drying overnight with calcium chloride. DOP was then vacuum-distilled (150 °C and 3 mmHg) and stored in a desiccator prior to use. Solutions were prepared gravimetrically, using methylene chloride as a cosolvent. The cosolvent was removed under a gentle flow of nitrogen, and then mild vacuum, until constant weight was achieved. Concentrations were converted to polymer volume fractions, ϕ, assuming additivity of volumes and a density of 0.981 g/mL for DOP. Each solution contained 0.1 wt % of polymer of the antioxidant BHT (2,6-di-*tert*-butyl-4-methylphenol) and was stored in a freezer at −20 °C to further inhibit degradation. Control samples prepared with and without BHT established that the additive had no discernible effect on the phase behavior. SEC was used to confirm that no degradation had taken place in samples that were exposed to temperatures above 175 °C.

Small-Angle X-ray Scattering. SAXS was used to confirm all ordered phase assignments. Measurements utilized Cu Kα X-rays (λ = 1.54 Å) from a Rigaku RTU-200BVH rotating anode, and Franks mirrors focused the beam onto an area detector (Siemens HI-STAR) placed about 2 m beyond the sample. Sample temperatures were mantained to within ±0.2 °C using a thermostated brass block. Two-dimensional images were corrected for detector response, azimuthally averaged, and placed on an intensity vs wavevector ($q = 4\pi \sin(\theta/2)/\lambda$) scale using duck-foot collagen to calibrate q. Typical exposure times varied from 1 to 20 min at each temperature. Samples were sealed under inert atmosphere in 1.5 mm quartz capillaries (Charles Supper Co.). Each solution was annealed for at least 5 min at a given temperature before measurements were taken, and were sometimes annealed for much longer periods out of the beam, to ensure structural equilibration.

Rheology. Rheological measurements were performed on an ARES instrument (Rheometric Scientific), using parallel plates of 25 or 50 mm diameter and gap widths of 0.5−1 mm. Care was taken to ensure that strain amplitudes were sufficiently small to remain within the linear viscoelastic regime. Possible effects of solvent evaporation and/or sample degradation were checked by repeating high-temperature measurements (note that the boiling point of DOP is ca. 384 °C). Measurements of the dynamic moduli G' and G'' were made in two modes: at a fixed low frequency (ω) as a function of temperature or as a function of ω at fixed temperature. The former protocol is well established as an effective means to locate order−order transitions (OOT) and the order−disorder transition (ODT)[1,20,22] and was so used extensively in this work. The typical frequency was below 1 rad/s, and the heating rate was ≤0.1 °C/min. The second protocol is useful for providing a preliminary identification of the morphology, as the low-frequency responses of the different phases have characteristic features.[23]

Static Birefringence. Static birefringence, or depolarization of transmitted light, has been established as a simple and convenient means to locate both OOTs and ODTs in block copolymer liquids.[16,20,24] Vertically polarized light from a HeNe laser passes through the sample and a horizontal analyzing polarizer onto a photodiode. Isotropic samples (i.e., disordered or cubic) do not depolarize light, and no signal is recorded, whereas lamellar or hexagonal phases are birefringent. In a typical experiment the solution is confined between glass disks and sealed with high-temperature adhesive and then subjected to a slow temperature increase (less than 1 °C/min). Each transition is indicated by the abrupt appearance or disappearance of significant transmitted intensity. Only ODTs from cubic phases could not be detected in this manner.

Results and Discussion

The phase diagrams (T vs polymer volume fraction, ϕ) will be presented in order of increasing styrene content, f. For each polymer, the measured ODTs (and OOTs where applicable) are indicated as distinct points, with smooth curves drawn to represent the assumed phase boundaries. As noted in the previous section, each transition was located by at least two of the three techniques (SAXS, rheology, and birefringence), with excellent agreement in all cases. Furthermore, each transition is reversible (except in one instance noted below). Also shown in each phase diagram are shaded areas, indicating the regions where the polystyrene glass transition inhibits equilibration.

In each plot a dashed curve is drawn, emanating from the melt ODT, which represents the dilution approxi-

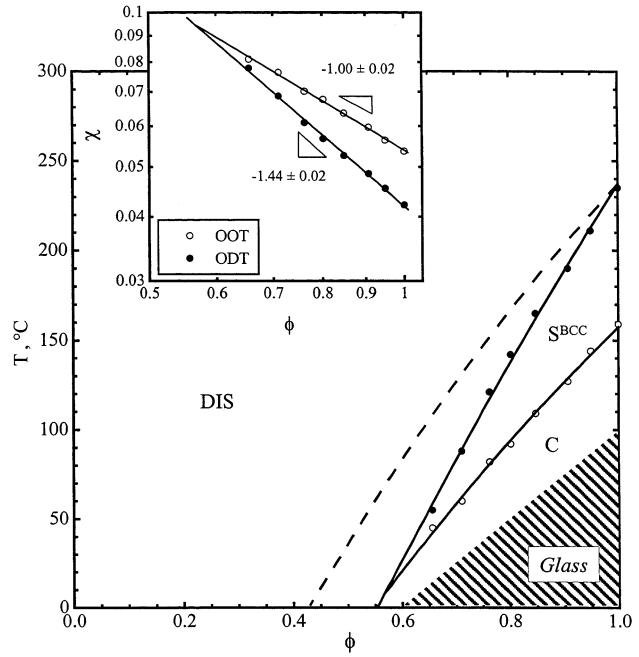

Figure 1. Phase diagram for SI(11−52) in DOP. Open circles denote measured OOTs, and filled circles denote ODTs. The dashed line represents the dilution approximation prediction for the ODT. The inset shows the ϕ dependence of χ for the ODT and OOT.

mation prediction for the ODT:

$$\chi_{ODT} \sim \phi^{-1} \tag{1}$$

This curve has been generated using the following expression for the temperature dependence of χ between PS and PI, based on a styrene segment reference volume:[16]

$$\chi = \frac{33}{T} - 0.0228 \tag{2}$$

In all cases this curve lies above the experimental ODT, indicating that the addition of neutral solvent is more effective at stabilizing the disordered state than mean-field theory anticipates. The same expression for χ is used to convert the measured transition temperatures into χ values, which are then plotted against ϕ as an inset to each phase diagram. The resulting curves are reasonably linear, indicating adherence to the general relation

$$\chi_{ODT} \sim \phi^{-\alpha} \tag{3}$$

where $\alpha = 1$ corresponds to the dilution approximation. The resulting exponent values are also noted in the insets.

Figure 1 shows the phase diagram for SI(11−52), which indicates a melt ODT from a body-centered array of spheres (S^{bcc}) at 235 °C and a cylinder (C) → S^{bcc} OOT at 159 °C. The ODT decreases more rapidly with added solvent than does the OOT, such that the two curves apparently intersect near $\phi \approx 0.6$. As can be seen from the inset, the OOT scaling follows the dilution approximation exactly within experimental uncertainty, whereas the ODT has $\alpha = 1.44$. Even though any uncertainty in $\chi(T)$ can affect the exact value of α, the differing concentration dependences of the two transitions is a robust experimental result and one that is not accounted for in mean-field theory. Figure 2 shows representative SAXS patterns for the $\phi = 0.76$ solution at various temperatures, which reveal the progression C → S^{bcc} → disorder (DIS) clearly.

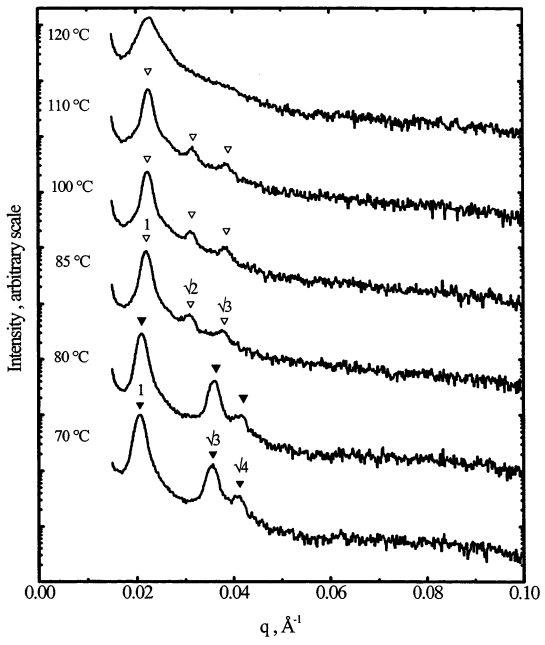

Figure 2. SAXS patterns (intensity vs wavevector, q) for SI(11−52), $\phi = 0.76$, at the indicated temperatures to illustrate the OOT and ODT. Arrows denote the characteristic reflections used to identify the ordered state symmetries. The individual curves have been shifted vertically for clarity.

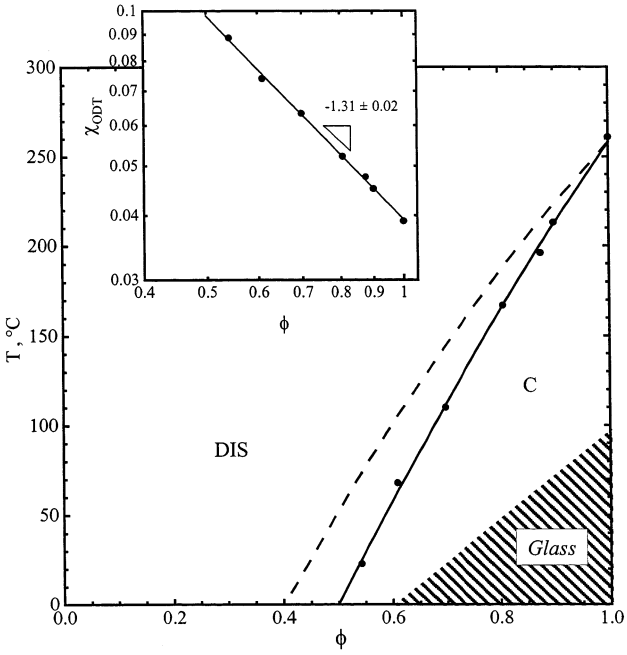

Figure 3. Phase diagram for SI(11−32) in DOP. The filled circles denote measured ODTs, and the dashed line represents the dilution approximation prediction for the ODT. The inset shows the ϕ dependence of χ for the ODT.

The preceding figures consider a copolymer at one extreme of the melt phase map, namely, a sample that exhibits S^{bcc} → DIS at the ODT. Figure 3 presents the phase diagram for SI(11−32), where the ODT corresponds to C → DIS at all concentrations. The dashed line again denotes the expected ODT curve based on the dilution approximation, and the inset quantifies the

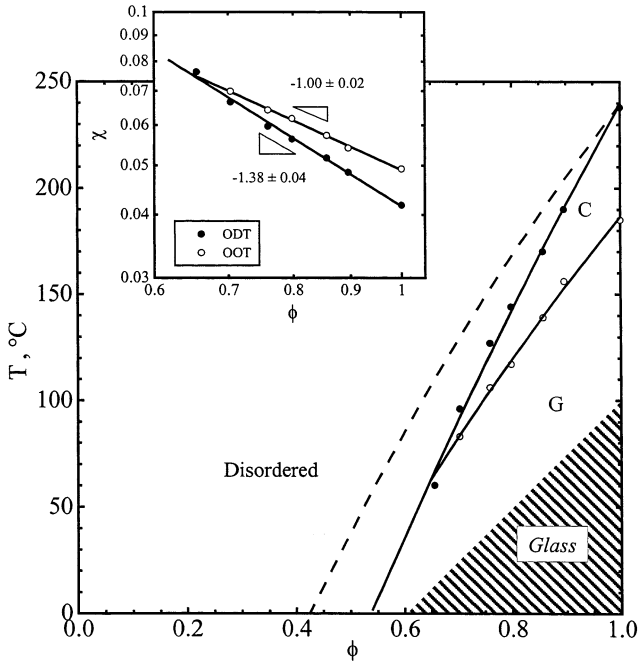

Figure 4. Phase diagram for SI(11−21) in DOP. Open circles denote measured OOTs, and filled circles denote ODTs. The dashed line represents the dilution approximation prediction for the ODT. The inset shows the ϕ dependence of χ for the ODT and OOT.

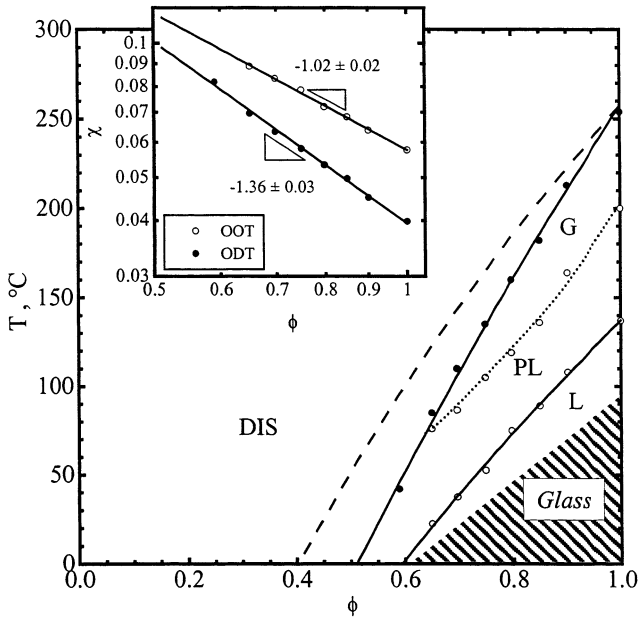

Figure 5. Phase diagram for SI(12−21) in DOP. Open circles denote measured OOTs, and filled circles denote ODTs. The dashed line represents the dilution approximation prediction for the ODT. The inset shows the ϕ dependence of χ for the ODT and OOT.

failure of that model; in this case $\alpha = 1.31$. It is worth recalling that even the presence of direct C → DIS transitions (and G → DIS and L → DIS shown subsequently) is not accommodated by mean-field theory, so fluctuations are presumably playing a significant role in both solutions and melts.

Figure 4 presents the corresponding results for SI(11−21), which shows a G → C OOT and a C → DIS ODT at high concentrations, which converge to a direct G → DIS ODT below $\phi \approx 0.65$. The scaling of the two transitions gives $\alpha = 1.00$ for the OOT and 1.38 for the ODT, in excellent agreement with the results in Figure 1. As the behavior of this particular sample in various solvents has been discussed in detail before,[18,19] we do not reproduce representative SAXS patterns of the various phases.

The copolymer SI(12−21) represents only a modest increase in f from SI(11−21) (i.e., from 0.31 to 0.33), but in this region of the phase diagram the equilibrium morphology is both predicted and found to be quite sensitive to f.[2,25−27] In this instance the sample exhibits L → G OOTs and G → DIS ODTs across the accessible concentration range, as shown in Figure 5. Consistent with SI(11−21) and SI(11−52), the OOT follows the dilution approximation ($\alpha = 1.02$) whereas the ODT does not ($\alpha = 1.36$). Representative SAXS traces for the $\phi = 0.70$ solution are shown in Figure 6. One complication arises in this particular sample, which is illustrated in Figure 5. Upon heating, the L phase first transforms to the metastable perforated layer phase (PL) and then to G. The fine dashed line represents an "apparent" OOT between PL and G, but in fact this boundary simply marks the point at which the kinetics of the metastable PL transforming to the equilibrium G are sufficiently rapid to occur on the measurement time scale. The metastability of PL relative to G has by now been established in many diblock copolymer systems, both melt and solution,[20,28−30] and has been demonstrated

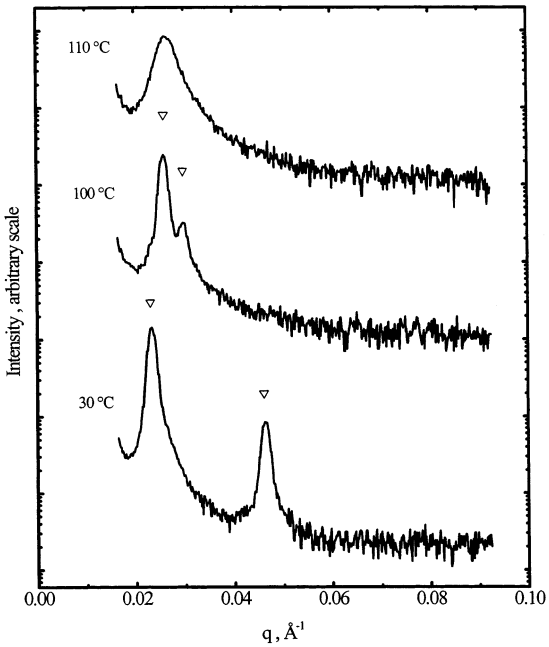

Figure 6. SAXS patterns (intensity vs wavevector, q) for SI(12−21), $\phi = 0.70$, at the indicated temperatures to illustrate the OOT and ODT. Arrows denote the characteristic reflections used to identify the ordered state symmetries. The individual curves have been shifted vertically for clarity.

theoretically.[26,31] We therefore take the observed L → PL transition as a good estimate of the underlying equilibrium L → G OOT.

The phase diagrams for SI(15−13), SI(22−12), SI(38−14), and SI(50−13) are shown in Figures 7−10, respectively. In these cases no OOTs are observed, and the ODTs correspond to L → DIS, L → DIS, C → DIS, and C → DIS, respectively. In all four systems the dilution approximation fails, with sequential α values of 1.38, 1.31, 1.53, and 1.60. We may therefore conclude that the failure of the dilution approximation to describe the

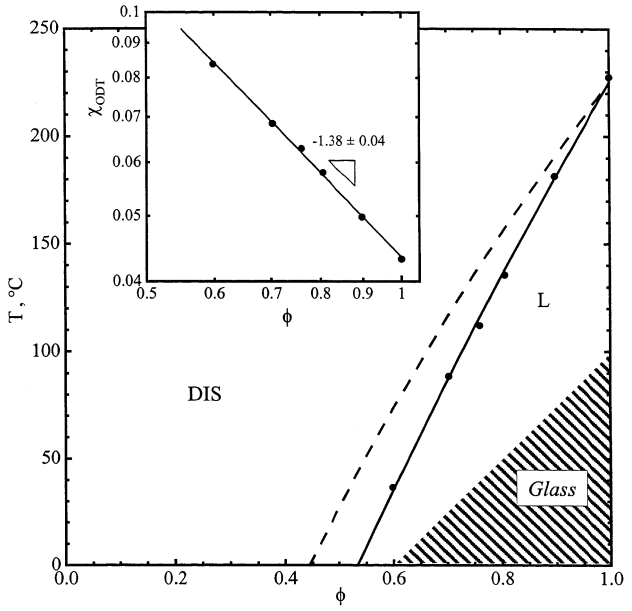

Figure 7. Phase diagram for SI(15−13) in DOP. The filled circles denote measured ODTs, and the dashed line represents the dilution approximation prediction for the ODT. The inset shows the ϕ dependence of χ for the ODT.

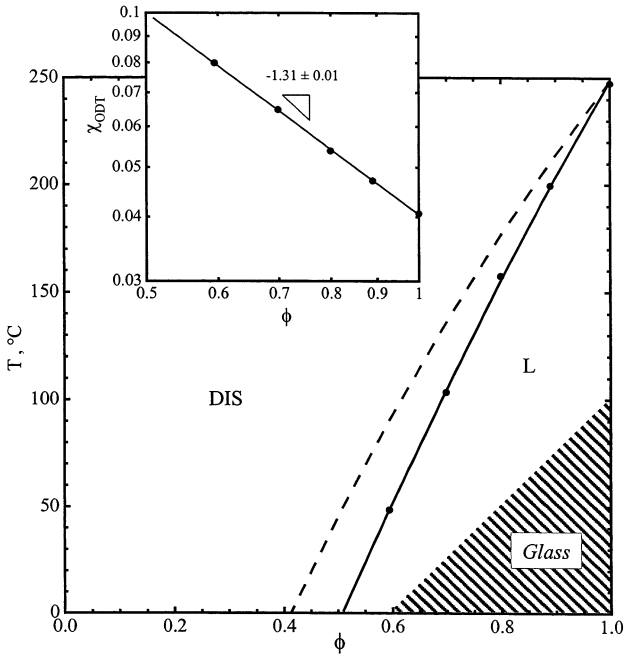

Figure 8. Phase diagram for SI(22−12) in DOP. The filled circles denote measured ODTs, and the dashed line represents the dilution approximation prediction for the ODT. The inset shows the ϕ dependence of χ for the ODT.

concentration dependence of the ODT for block copolymers in neutral solvents, previously established for lamellar samples,[16] extends to copolymers of all compositions. In contrast, the concentration dependence of OOTs conforms precisely to the dilution approximation, within experimental error. This result was first noted for a system displaying a G → C OOT[18] and is here extended to L → G (or PL) and C → S^{bcc}. A quantitative theoretical description of these results is lacking (as is also the case for the experimental ODT in melts), but nevertheless the important factors can be identified. The failure of mean-field theory to predict the experimental ODT in melts resides primarily in an inaccurate de-

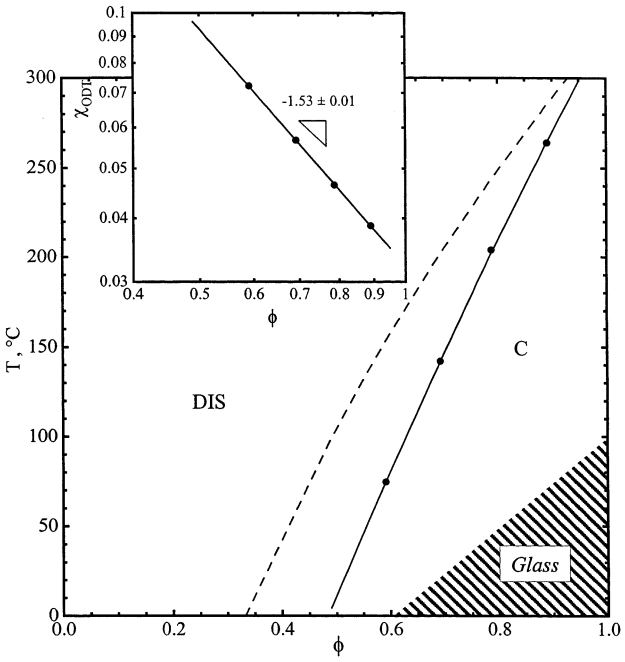

Figure 9. Phase diagram for SI(38−14) in DOP. The filled circles denote measured ODTs, and the dashed line represents the dilution approximation prediction for the ODT. The inset shows the ϕ dependence of χ for the ODT.

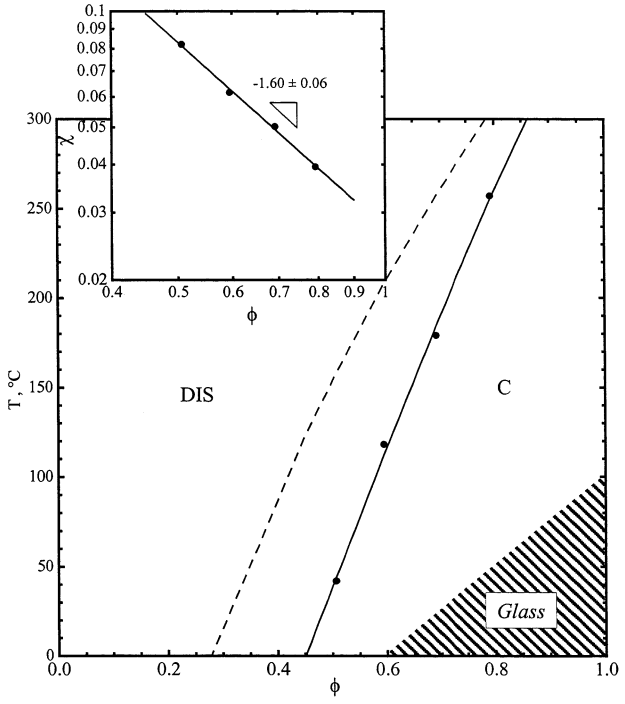

Figure 10. Phase diagram for SI(50−13) in DOP. The filled circles denote measured ODTs, and the dashed line represents the dilution approximation prediction for the ODT. The inset shows the ϕ dependence of χ for the ODT.

scription of the disordered state free energy. (The fluctuation theory of Fredrickson and Helfand,[8] which adapts the Brasovskii[32] approach to the underlying mean-field theory of Leibler,[33] anticipates much of the associated phenomenology but is limited in its quantitative applicability to smaller fluctuation effects than are typically encountered. Liquid state theories, such as the PRISM approach,[9,10,21] may offer more promise in this regard but are nonetheless restricted in their ability to locate the ODT.) The experimental results suggest that

the mean-field estimate of the disordered state free energy is even less reliable than in the melt; this is certainly plausible on the basis of the relative success of Flory−Huggins theory in describing the phase behavior of polymer melt blends vs solutions. Apparently, polymer solvent fluctuations supplement the already strong polymer composition fluctuations to stabilize the disordered solution to increasingly greater extents. The success of the dilution approximation in describing the concentration dependence of OOTs is completely consistent with this picture. In this case, mean-field theory relies on a comparison of the free energies of two ordered states, both of which are computed rather reliably. In short, once within the boundary of the order−disorder transition, the full SCMF is a reliable guide to the phase behavior of block copolymer solutions as well as melts.

In the context of the first question posed in the Introduction, whether the topology of the melt phase map is preserved upon dilution with a neutral solvent, the results presented here indicate that the answer is both "yes" and "no". In terms of the morphologies observed, and the composition dependence of the phase boundaries relatively far from the ODT, the dilution approximation holds. However, near the ODT, where the melt phase boundaries curve strongly in the χN vs f map, the effect of dilution with a neutral solvent is more complicated. In essence, dilution expands the domain of stability of the disordered state, to the extent that some ordered phases observed at the ODT in the melt are progressively "eroded" away by added solvent.

It is worth noting two possible factors that might be considered, but that in fact are not playing a significant role. First, the spatial distribution of solvent within the ordered state conforms to the predictions of mean-field theory. In particular, a neutral solvent is distributed essentially homogeneously within the two microdomains, except for a slight accumulation at the styrene−isoprene interfaces, as we have previously demonstrated using SANS and deuterated solvents.[34,35] Second, the elevated values of α might suggest that chain swelling is playing a significant role, as values of $\alpha \approx 1.6$ are anticipated in semidilute solution. However, the concentrations employed here are all greater than 0.5, which are too large for significant excluded-volume effects on chain dimensions. Furthermore, there is no hint of a crossover to a mean-field scaling as $\phi \rightarrow 1$ in any of the systems studied.

It is of interest to enquire whether the values of α display any discernible trends. As noted in the Introduction, we have previously demonstrated a system dependence for lamellar samples: $\alpha \approx 1.6$ in PS−PI but $\alpha \approx 1.2$ for PEP−PEE.[16] This nonuniversality emerges as a natural consequence of local packing constraints in the PRISM model.[10,21] The values of α reported here are collected in Figure 11 and plotted against N. There is some suggestion that α increases with N, which is somewhat counterintuitive; one might expect the behavior to become more mean-field-like in the large N limit. However, the value of N employed for PEP−PEE was distinctly larger than those here, but $\alpha \approx 1.2$, so it is not clear whether this trend is significant. We also point out that there is no obvious correlation of α with composition, and so the data are not plotted in this manner.

The final issue we wish to consider is the scaling of the domain spacing, d, with ϕ and χ. This particular subject has been studied in some detail by Hashimoto and co-workers for SI copolymers in DOP, in both the ordered and disordered states,[12,13,36] and consequently our discussion can be brief. The results for four polymers are presented in Figure 12 as $d/\phi^{1/3}$ vs χ in a double-logarithmic format. The four polymers represent the four different symmetries, such that for SI(11−52) $d = d_{110}$ (S^{bcc}), for SI(11−32) $d = d_{100}$ (C), for SI(11−21) $d = d_{211}$ (G), and for SI(51−13) $d = d_{100}$ (L). For each polymer the data collapse well to a smooth line, justifying the assumed scaling with $\phi^{1/3}$. The dependence on χ is also seen to be well represented by a power law, with exponents ranging from 0.23 to 0.31. The SCMF calculations of Whitmore and Noolandi finds that d scales approximately as $\phi^{0.22}$ in stronger segregation (large N, $\phi \rightarrow 1$), evolving smoothly to $d \sim \phi^{0.38}$ as the ODT is approached.[6] Similarly, they find $d \sim \chi^{0.2}$ in stronger segregation, and $d \sim \chi^{0.33}$ in the vicinity of the ODT. Consequently, our experimental results are in excellent

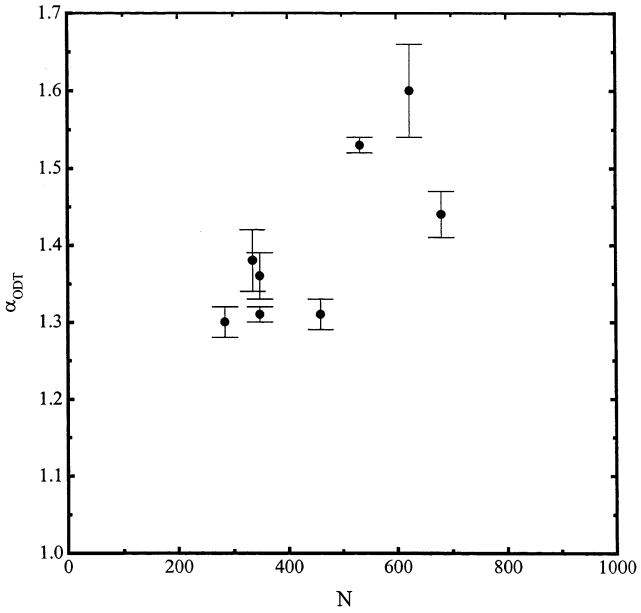

Figure 11. Exponent (α) for the ϕ dependence of χ at the ODT vs total degree of polymerization N.

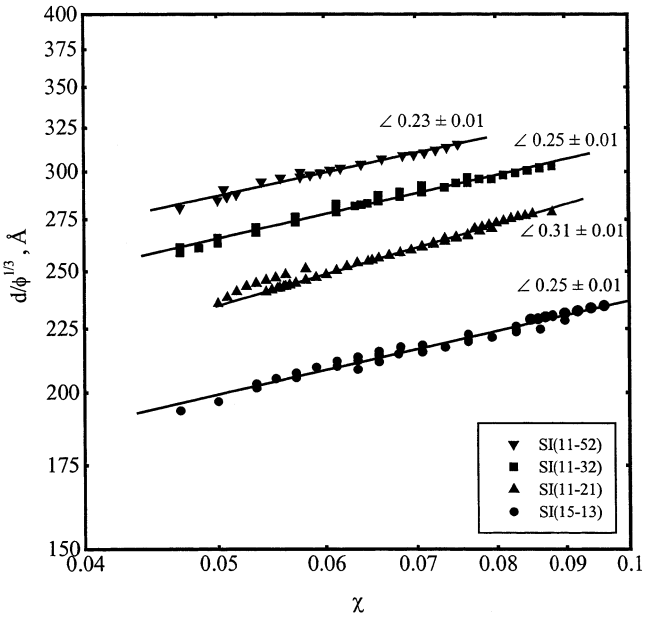

Figure 12. Characteristic d spacing, normalized by $\phi^{1/3}$, vs χ for the indicated polymers.

agreement with these calculations. Furthermore, they agree well with the data of Hashimoto and co-workers, where $d \sim (\phi\chi)^{1/3}$ over a comparable range of segregation strengths.[12,13,36] However, these exponents should be contrasted to the strong segregation limiting result of $d \sim (\phi\chi)^{1/6}$.[3,37]

The adherence of the experimental behavior of d in the ordered state to the predictions of the SCMF theory may be attributed to the same factors that lead to the success of the dilution approximation in describing the ϕ dependence of order−order transitions, namely, that the mean-field theory computes the relative free energies and structural details of the various ordered phases extremely well. However, the results of Hashimoto and co-workers for $d(\phi,\chi)$ span both the ordered and disordered states, and a consistent description is obtained by taking an effective interaction parameter proportional to $\phi\chi$.[13] This implies that the dilution approximation is also successful in accounting for the concentration dependence of the local interactions. We believe that these results underscore the fact that the failure of the dilution approximation to describe the order−disorder transition correctly is due to a miscalculation of the disordered state free energy. In this sense the PRISM approach may be a more promising route to a quantitative description, as it emphasizes the disordered side of the phase boundary.[10,21]

Summary

The phase behavior of diblock copolymers in a neutral solvent has been mapped out as a function of f, ϕ, and T. The results may be summarized in terms of their adherence to or disagreement with the expectations of mean-field theory in general, and the dilution approximation in particular. The most important result is that the order−disorder transition does not follow the dilution approximation ($\chi_{ODT} \sim \phi^{-1}$) for any copolymer composition. Rather, $\chi_{ODT} \sim \phi^{-\alpha}$ with $\alpha \approx 1.3-1.6$. This phenomenon can be broadly attributed to additional fluctuation stabilization of the disordered state upon addition of a second, lower molar mass component. On the other hand, three different order−order transitions did consistently follow the dilution approximation scaling, $\chi_{OOT} \sim \phi^{-1}$, which is attributable to the success of the mean-field theory in computing the relative free energies of the various ordered states. As a consequence of these different scalings with concentration, the phase diagram in the vicinity of the ODT is qualitatively different in neutral solution than in the melt. For a given composition, the addition of solvent progressively "erodes" the phase nearest the ODT, which can ultimately "expose" another phase and thereby change the nature of the ODT. Finally, for all four symmetries (lamellae, gyroid, hexagonal cylinders, and body-centered-cubic spheres) the principal domain spacing scales with ϕ and χ in agreement with self-consistent mean-field calculations and with previous experiments.

Acknowledgment. This work was supported by the National Science Foundation through Awards DMR-9528481 and DMR-9901087 as well as through the University of Minnesota MRSEC (DMR-9809364).

References and Notes

(1) Hamley, I. W. *The Physics of Block Copolymers*; Oxford University Press: Oxford, 1998.
(2) Bates, F. S.; Fredrickson, G. H. *Annu. Rev. Phys. Chem.* **1990**, *41*, 525.
(3) Helfand, E.; Tagami, Y. *J. Chem. Phys.* **1972**, *56*, 3592.
(4) Hong, K. M.; Noolandi, J. *Macromolecules* **1983**, *16*, 1083.
(5) Whitmore, M. D.; Noolandi, J. *J. Chem. Phys.* **1990**, *93*, 2946.
(6) Whitmore, M. D.; Vavasour, J. D. *Macromolecules* **1992**, *25*, 2041.
(7) Huang, C.-I.; Lodge, T. P. *Macromolecules* **1998**, *31*, 3556.
(8) Fredrickson, G. H.; Helfand, E. *J. Chem. Phys.* **1987**, *87*, 697.
(9) David, E. F.; Schweizer, K. S. *J. Chem. Phys.* **1994**, *100*, 7767.
(10) Guenza, M.; Schweizer, K. S. *J. Chem. Phys.* **1997**, *106*, 7391.
(11) Jin, X.; Lodge, T. P. *Rheol. Acta* **1997**, *36*, 229.
(12) Mori, K.; Okawara, A.; Hashimoto, T. *J. Chem. Phys.* **1996**, *104*, 7765.
(13) Mori, K.; Hasegawa, H.; Hashimoto, T. *Polymer* **2001**, *42*, 3009.
(14) Fredrickson, G. H.; Leibler, L. *Macromolecules* **1989**, *22*, 1238.
(15) Olvera de la Cruz, M. *J. Chem. Phys.* **1989**, *90*, 1995.
(16) Lodge, T. P.; Pan, C.; Jin, X.; Liu, Z.; Zhao, J.; Maurer, W. W.; Bates, F. S. *J. Polym. Sci., Polym. Phys. Ed.* **1995**, *33*, 2289.
(17) Lodge, T. P.; Xu, X.; Ryu, C. Y.; Hamley, I. W.; Fairclough, J. P. A.; Ryan, A. J.; Pedersen, J. S. *Macromolecules* **1996**, *29*, 5955.
(18) Hanley, K. J.; Lodge, T. P. *J. Polym. Sci., Polym. Phys. Ed.* **1998**, *36*, 3101.
(19) Hanley, K. J.; Lodge, T. P.; Huang, C.-I. *Macromolecules* **2000**, *33*, 5918.
(20) Lodge, T. P.; Pudil, B.; Hanley, K. J. *Macromolecules* **2002**, *35*, 4707.
(21) Guenza, M.; Schweizer, K. S. *Macromolecules* **1997**, *30*, 4205.
(22) Fredrickson, G. H.; Bates, F. S. *Annu. Rev. Mater. Sci.* **1996**, *26*, 503.
(23) Zhao, J.; Majumdar, B.; Schulz, M. F.; Bates, F. S.; Almdal, K.; Mortensen, K.; Hajduk, D. A.; Gruner, S. M. *Macromolecules* **1996**, *29*, 1204.
(24) Balsara, N. P.; Perahia, D.; Safinya, C. R.; Tirrell, M.; Lodge, T. P. *Macromolecules* **1992**, *25*, 3896.
(25) Matsen, M. W.; Bates, F. S. *Macromolecules* **1996**, *29*, 1091.
(26) Matsen, M. W.; Bates, F. S. *Macromolecules* **1996**, *29*, 7641.
(27) Bates, F. S.; Schulz, M. F.; Khandpur, A. K.; Förster, S.; Rosedale, J. H.; Almdal, K.; Mortensen, K. *J. Chem. Soc., Faraday Discuss.* **1994**, *98*, 7.
(28) Hajduk, D. A.; Takenouchi, H.; Hillmyer, M. A.; Bates, F. S.; Vigild, M. E.; Almdal, K. *Macromolecules* **1997**, *30*, 3788.
(29) Vigild, M. E.; Almdal, K.; Mortensen, K.; Hamley, I. W.; Fairclough, J. P. A.; Ryan, A. J. *Macromolecules* **1998**, *31*, 5702.
(30) Wang, C.-Y.; Lodge, T. P. *Macromol. Rapid Commun.* **2002**, *18*, 49.
(31) Qi, S.; Wang, Z.-G. *Macromolecules* **1997**, *30*, 4491.
(32) Brazovskii, S. A. *Sov. Phys. JETP* **1975**, *41*, 85.
(33) Leibler, L. *Macromolecules* **1980**, *13*, 1602.
(34) Lodge, T. P.; Hamersky, M. W.; Hanley, K. J.; Huang, C.-I. *Macromolecules* **1997**, *30*, 6139.
(35) Huang, C.-I.; Chapman, B. R.; Lodge, T. P.; Balsara, N. P. *Macromolecules* **1998**, *31*, 9384.
(36) Shibayama, M.; Hashimoto, T.; Hasegawa, H.; Kawai, H. *Macromolecules* **1983**, *16*, 1427.
(37) Semenov, A. N. *Sov. Phys. JETP* **1985**, *61*, 733.

MA0209601